Nanomedicine: Nanotechnology, Biology, and Medicine
22 (2019) 102108

nanomedicine
Nanotechnology, Biology, and Medicine

nanomedjournal.com

Purinergic receptor (P2X7) activation reduces cell–cell adhesion between tubular epithelial cells of the proximal kidney

Eleftherios Siamantouras, PhD, Gareth W. Price, PhD, Joe A. Potter, PhD, Claire E. Hills, PhD, Paul E. Squires, PhD*

Joseph Banks Laboratories, School of Life Sciences, Green Lane, University of Lincoln, UK

Revised 6 October 2019

Abstract

Loss of epithelial (E)-cadherin mediated cell–cell adhesion impairs gap junction formation and facilitates hemichannel-mediated ATP release in the diabetic kidney. Linked to inflammation and fibrosis, we hypothesized that local increases in inter-cellular ATP activate P2X7 receptors on neighboring epithelial cells of the proximal tubule, to further impair cell–cell adhesion and ultimately exacerbate tubular injury. Immunoblotting confirmed changes in E-cadherin expression in human kidney cells treated with non-hydrolysable ATPγS ± the P2X7 antagonist, A438079. Atomic force microscopy based single-cell force spectroscopy quantified maximum unbinding force, tether rupture events, and work of detachment. Confocal microscopy assessed cytoskeletal reorganization. Our studies confirmed that ATPγS downregulated E-cadherin expression in proximal kidney cells, loss of which was paralleled by a reduction in intercellular ligation forces, decreased tether rupture events and cytoskeletal remodeling. Co-incubation with A438079 restored loss of adhesion, suggesting that elevated extracellular ATP mediates tubular injury through P2X7 induced loss of E-cadherin mediated adhesion.

Key words: Kidney; Adherens junction; Cell adhesion; ATP; P2X7; AFM-SCFS

Diabetic nephropathy is the leading cause of End Stage Renal Disease (ESRD) in people with diabetes.[1] Characterized by multiple structural and functional disturbances, tubulointerstitial fibrosis of the proximal region of the kidney represents a major underlying pathology of diabetic nephropathy and develops in response to a number of morphological and phenotypic changes.[2] We have previously reported that glucose-evoked increases in the beta1 isoform of the profibrotic cytokine Transforming Growth Factor (TGFβ1), drive a loss of epithelial associated markers, with a concomitant increase in proteins more commonly associated with fibroblasts.[3] Often referred to as partial epithelial-to-mesenchymal transition (pEMT), this series of events is initiated in response to impaired expression of epithelial (E)-cadherin and the functional loss of cell–cell adhesion.[4–6] Decreased cell–cell adhesion prevents docking of connexons on adjacent membranes and decreases Gap Junction-mediated Intercellular Communication (GJIC).[7] In the absence of neighboring binding partners, uncoupled connexons form hemichannels that release nucleotides, e.g. adenosine triphosphate (ATP), in to the intercellular space.[8] Locally released ATP binds purinoceptors, notably P2X7, and is linked to the progression and development of inflammation and fibrosis in multiple tissue types,[9–11] including the diabetic kidney.[12–15] With our recent studies linking increased hemichannel mediated ATP release to both inflammation and fibrosis, it seems likely that increased intercellular ATP may accelerate progression of tubular injury by exacerbating the further loss of cell–cell tethering.

Part of the multi-protein adherens junction (AJ), cadherins are calcium-dependent trans-membrane cell adhesion proteins that connect the cell interface to actin cytoskeleton (CSK). The extracellular domains of individual cadherins form weak (40pN) binding pairs[16] with cadherins on adjacent cells, while the cytoplasmic domain bind β-catenin, linking cadherins to the cytoskeleton via α-catenin.[17,18] By regulating ligation clustering, interaction of cadherin with F-actin, via catenins, is crucial

Funding: This work was supported by a Diabetes UK equipment grant for the AFM-SCFS (12/0004546). ES was supported by EFSD/Boehringer Ingelheim European Research Programme in Microvascular Complications of Diabetes (CEH & PES); GWP (16/0005427, PES & CEH) and JAP (16/0005544) were supported by Diabetes UK.

*Corresponding author at: Joseph Banks Laboratories, School of Life Sciences, University of Lincoln, Lincoln, Lincolnshire, LN6 7DL, United Kingdom.

E-mail address: PSquires@lincoln.ac.uk. (P.E. Squires).

https://doi.org/10.1016/j.nano.2019.102108

in maintaining adhesive strength and acts as a signaling 'node' for proteins that influence adhesiveness &/or initiate intracellular signaling.[19,20] In recruiting catenins, cadherins trigger signals that modulate the actin cytoskeleton at the point of cell–cell contact.[21]

The intricate molecular structure of the adherens junction and viscoelastic properties of the cytoskeleton suggest that separation of adherent cells is a complex process. Recent efforts to systematically investigate the effects of mechano-chemical changes in cell–cell adhesion in diabetic nephropathy[6] and other pathological states have been reported.[22–24] It is clear that the assembly of AJs in correlation with the intrinsic physical properties of adherent cells drive a complex separation process. Force spectroscopy of cell–cell detachment is a powerful method that can be used to capture the biophysical response of molecular units at a nanoscale resolution. However, comprehensive analysis of force-displacement (*F-d*) curves is required, since *F-d* retraction curves between cells can be used to observe the collective behavior of the surface ligation clustering and the CSK-AJ domain. Clustering of cadherins is associated with increased actin polymerization, a process that enhances the assembly of the AJ and maintains stability of cell–cell adhesion.[25] Evidence suggests that prior to clustering, cadherins associate with the catenin domain and that the clustering is organized by the actin cytoskeleton.[18,19] Cell–cell contact formation is typically followed by contact maturation and in epithelial cells, precedes the formation of tight junctions. A nanoscale study by Wu et al (2015) showed that E-cadherin clusters never increased in size or merged to drive changes in architecture and adhesion, instead their organization in clusters was regulated by the cytoskeleton, highlighting its significant role in the assembly of distinct nanoscale ligation clusters. Multi-variable analysis of nanoscale *F-d* separation process between cells can address the functional changes of distinct ligation components after treatment with a biochemical stimulus.

Although initially used to study molecular function of binding receptors,[26] AFM-based force spectroscopy has been applied to investigate the separation behavior of whole cells.[27,28] In the current study we applied AFM-based single-cell force spectroscopy (SCFS) to investigate the effects of ATP in mediating loss of adhesion between tubular epithelial cells of the proximal kidney via P2X7 purinoceptors. The AFM-based instrument incorporates an extended displacement range (100 μm) to allow complete separation of adherent cells for nanoscale resolution. Our novel analytical data clarify the mechanism by which the loss of cell–cell adhesion is regulated by the physicochemical interplay between the extracellular and intracellular domains of E-cadherin, and provide compelling evidence that ATP-mediated paracrine signaling is important in progression of early tubular injury in kidney disease.

Methods

Reagents

Fibronectin and ATPγS were obtained from Sigma (Poole, UK). P2X7 receptor antagonist A438079, tetramethyl rhodamine isothiocyanate (TRITC)-conjugated phalloidin, DAPI (4′,6-diamidino-2-phenylindole) and goat serum were purchased from Bio-Techne (Abingdon, UK). Immobilon-Fl PVDF membrane was from Millipore (Watford, UK), while Odyssey blocking buffer and secondary fluorescent antibodies were purchased from LI-COR (Cambridge, UK). Anti-E-cadherin was purchased from Cell Signalling Technologies (Hertfordshire, UK), while alpha-tubulin was purchased from Sigma (Poole, UK).

Culture of HK2 cells

Human derived proximal tubule kidney (HK2) epithelial cells were purchased from the American Type Culture Collection (ATCC; Gaithersburg, MD 20878). Tissue culture media and plasticware were from Invitrogen Life Technologies (Paisley, UK). HK2 cells (passage 18-30) were maintained in DMEM/Ham's F12 (DMEM/F12) medium, `supplemented with 10% fetal calf serum (FCS), glutamine (2 mmol/l), 2% penicillin–streptomycin, and epidermal growth factor (EGF; 5 ng/ml). Cells were seeded onto 40 mm petri-dishes, T25 flasks (for suspended cells) and cultured at 37 °C in a humidified atmosphere of 5% CO_2 in air. Prior to treatment, cells were cultured in DMEM/F12 low glucose (5 mM) for 48 h. Basal (5 mM) glucose culture media were generated as described previously.[3] Cells were then treated with ATPγS (100 μM) + A438079 (50 μM) for 48 h. In all experiments, cells were serum starved overnight before stimulation.

Western blotting

Preparation of protein, its separation by SDS-gel electrophoresis and transfer onto Immobilon-Fl PVDF membranes have been described previously.[3] Membranes were blocked with Odyssey blocking buffer overnight (LI-COR), then probed simultaneously with a polyclonal antibody against E-cadherin (1:1000) and alpha-tublin (1:20,000) for 1 h at room temperature. Bands were visualized using an Odyssey FC and semi-quantified using Image Studio (v5.2, LI-COR).

AFM single-cell force spectroscopy

AFM is a powerful tool for high-resolution single cell force measurements. Briefly, a piezo actuator moves the base of a cantilever towards the surface of the sample in the vertical direction and then retracts it again, while the deflection of the cantilever is measured continuously. An SCFS force curve is the result of mechanical interaction between the tip of the cantilever and the surface of the sample. When the cantilever is retracted from the sample adhesion occurs, in which the cantilever is still in contact with the sample. During this process the cantilever is deflected downwards, and adhesion can be detected in a force curve by a negative force peak (Figure 1). As the cantilever is further retracted from the surface, adhesion forces will be disrupted, and the tip will be completely separated from the sample. Using spring stiffness, the deflection of the cantilever provides information about the elastic properties of the sample and a direct measure of the adhesion forces. Force spectroscopy between single, soft biological cells includes more complex interactions between the tip and the sample. As the cantilever is retracted, hysteresis is observed, which is common for

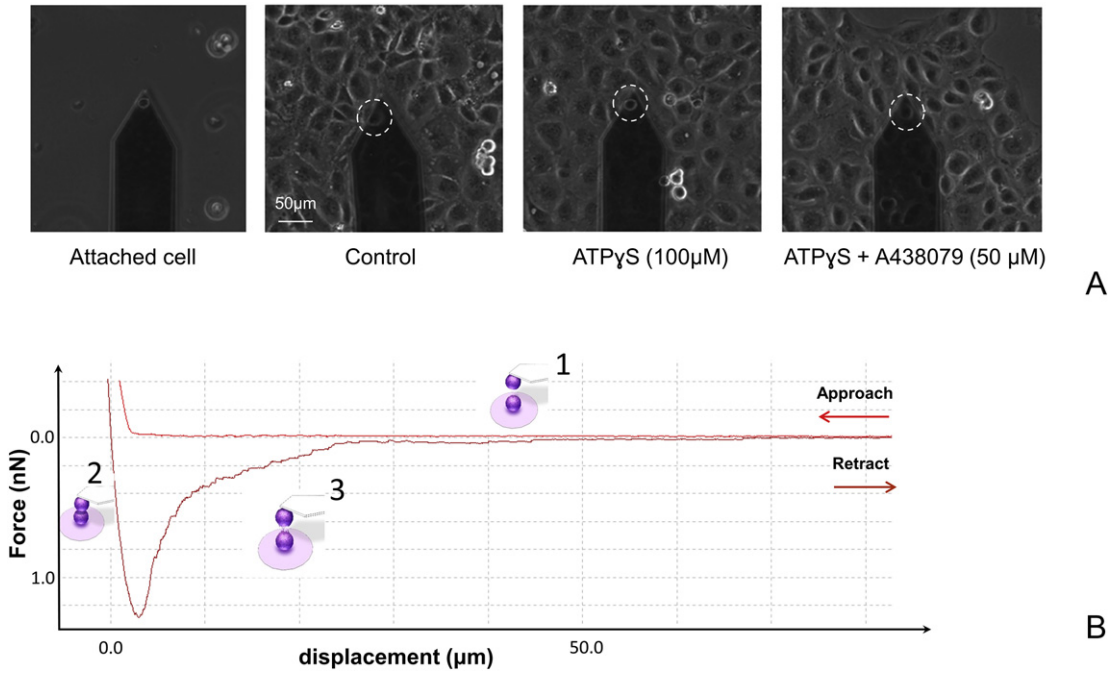

Figure 1. (**A**) Phase microscopy images of probe cells attached on the cantilever from each treatment. Clusters of treated cells are firmly attached in the substrate. The probe cell was brought in contact above the central point of the nucleus for 10 s with a contact force of 1 nN. The probe cell was then retracted at a 5 μm/s while force vs displacement was continuously recorded. (**B**) A retraction *F-d* curve of a control cell illustrating the experimental process. In phase 1 the probe cell is moving vertically downwards until the preset force is reached. During phase 2, interaction between the two cells occurs in which ligation is formed. Lastly, in phase 3 the probe cell is retracted until the force returns to the baseline where the two cells are separated.

viscoelastic materials. In addition, adhesion of the tip with long surface molecules requires an extended displacement range to avoid extendable contacts. The cantilever-attached cell was brought in contact with substrate-attached cell, until a pre-set contact force of 1nN was reached. The cells were allowed to form ligation during a contact time of 10 s, after which the cantilever was retracted using a velocity 5 μm/s until the two cells were completely separated. The procedure was repeated three times for each cell tested, with 45 s intervals between each measurement. Velocity was kept constant during the extend and retract processes. Data were collected from three separate experiments (n = 3).

Instrumentation

Latest advancements in AFM-force spectroscopy allow for an effective displacement range (100 μm), sufficient to disrupt adhesion forces needed for complete cell separation and facilitate the investigation of cell-to-cell contact. Experiments were performed using the CellHesion®200 module (JPK Instruments, Berlin, Germany) that was installed on an Eclipse TE 300 inverted microscope (Nikon, USA). During each experiment, cells were maintained at 37 °C by incorporating the BioCell™ temperature controller (JPK, Berlin, Germany) into the AFM stage. Phase microscopy images were acquired using a CCD camera (Orca, Hamamatsu) connected on the side port of the microscope. To avoid hydrodynamic drag when performing *F-d* curves in liquid a speed of 5 μm/s was used. The AFM-SCFS set-up with the CCD camera was driven by JPK's CellHesion200 software. Images were captured at ×20 magnification. The system was supported on an anti-vibration table (TMC 63-530, USA). Changes in the temperature of the room were less than 0.5-1 °C during experimental measurements. Deflection of the cantilever was measured by the difference in the reflection of a laser beam between the upper or lower parts a quadric-sected photodiode.

Functionalization

To perform cell–cell adhesion experiments, suspended cells were introduced into the media of testing cells and a single cell was attached on a tipless cantilever. An arrow geometry is designed to ease manipulation of individual cells among others in close proximity. Arrow sensors (TL1, Nanoworld AG, Switzerland) with force constant of 0.03 N/m were used to attach cells to the free end of the sensor. Tipless cantilevers are more suitable for adhesion experiments since any contact of the tip with the surface of the cell or the substrate will disrupt the measurements. The attached cell was probing an adherent cell on the substrate in order to investigate the disruption forces between two cells. Tip-less cantilevers were chemically functionalized so that a single suspended cell could be attached. Initially the cantilevers were sterilized by UV treatment (10mins). Next, they were incubated in poly-L-lysine (25 μg/ml in PBS) for 30mins at room temperature (RT). Subsequently, the cantilevers were transferred in fibronectin solution (20 μg/ml in PBS) and they were incubated for 2 h at 37 °C. After functionalization cantilevers were stored in PBS solution at 4 °C and used within 3 days.

Calibration

For small deflections the cantilever approximates a Hookean spring, hence the deflection is linearly related to the acting force. When the cantilever spring constant is calculated, the deflection can be converted into the corresponding force ($F = k*x$). Each functionalized cantilever was calibrated prior to experimentation to determine the actual spring constant value, using the manufacturer's software (JPK Instruments, Germany) based on the thermal noise amplitude.[29,30] This method measures the thermal fluctuations of the cantilever deflection and uses the equi-partition theorem to calculate the cantilever spring constant. Initially the deflection of the cantilever is displayed as the output of the photodetector in Volts (>1 V). To record a force curve for calibration, the cantilever was configured to approach the base of a cell-free petri-dish once, to minimize the loss of coating (set-point <1 V). This linear curve was used to determine sensitivity, or the distance of cantilever deflection for a given voltage difference measured by the photodiode, which was below 100 nm/V for all cantilevers used. The amplitudes of the thermal fluctuation were measured at 37 °C. Since the calibration process was conducted in culturing media a correction factor of 0.251 was used.[30] The mean spring constant was 0.02024 N/m, range: 0.0098, STD: 0.00348. The position of the cantilever on the glass holder and the alignment parameters were maintained throughout experiments as any disturbance would result in re-calibration.

Immunocytochemistry

Cells were seeded onto glass-coverslips (22 mm diameter) in low glucose (5 mM) for 48 h, serum-starved overnight, and then incubated with ATPγS (100 μM) ± A438079 (50 μM) for 48 h. Cells were fixed with 4% paraformaldehyde, blocked with goat serum, and stained with DAPI (1 mmol/l) for 3 min, before being incubated with tetremethyl rhodamine isothiocyanate (TRITC)-conjugated phalloidin (1:400 in PBS-Triton) for 1 h. Cells were visualized using an inverted Leica confocal microscope, using a hybrid Leica HyD detector. Leica Application Suite X (LAS X) software was used to operate the confocal hardware and overlay resulting images.

Data processing and analysis

Three force-displacement curves were acquired per cell during experiments and were processed using the JPK data processing software. The separation parameters analyzed in this study are the maximum unbinding force F_{max}, the work of detachment W_d and the number of tether rupture events (TREs). To signify statistical significances data were evaluated using univariate ANOVA followed by Tukey's multiple comparisons post-test using SPSS (version 24). Data from SCFS are expressed as mean ± SEM in the text and as median and quartile range at the graphs. Sample numbers refer to separate cell passages made up of recordings from multiple individual cells and are represented with '*n*' for passage number. $P < 0.05$ was taken to indicate statistical significance.

Results

ATPγS downregulates E-cadherin expression via activation of P2X7 receptors

We recently demonstrated that glucose-evoked changes in TGF-β1 evoked cytoskeletal remodeling and reduced cellular adhesion,[6] events that culminated in a loss of gap junction intercellular communication and increased hemichannel mediated ATP release.[8] To determine whether ATP propagates this process, HK2 cells were cultured in 5 mM glucose for 48 hr., serum-starved overnight, and subsequently incubated with the non-hydrolysable ATPγS (100 μM) for 48 h. In control cells, TRITC-conjugated phalloidin confirmed that the actin cytoskeleton was made up of a diffuse transcellular network of F-actin filaments that spanned the cytosol. Treatment with ATPγS produced denser peripheral stress fibers (Figure 2, *A*), an effect reversed when co-incubated with the P2X7 antagonist A438079 (50 μM). Immunoblotting confirmed that ATPγS decreased whole-cell expression of E-cadherin to 54.4 ± 4% (Figure 2, *B*; $P < 0.01$, $n = 3$), an effect reversed when HK2 cells were co-incubated with ATPγS (100 μM) and the selective P2X7 inhibitor, A438079 (50 μM, 113.6 ± 9.7%; Figure 2, *B*; $n = 3$),

ATPγS decreases maximum unbinding force (F_{max}) via activation of P2X7 receptors

AFM-based single cell force spectroscopy (SCFS) was used to quantify the unbinding forces required to separate two cells. The minimum negative point during the pulling phase of the *F-d* curve represents the maximum downward deflection of the cantilever as the probe cell is retracted from the substrate cell in the vertical axis. Therefore, the minimum force value of a retraction curve corresponds to the maximum unbinding force F_{max} (Figure 3, *B*). Nanoscale forces are correlated with any alteration in the number of E-cadherin ligations and the associated formation of clusters that promote adhesion. Using SCFS the maximum unbinding forces were quantified after P2X7 activation. Force and contact time remained constant throughout the experiments, while the approach–retract cycle was repeated three times for each cell. To determine F_{max}, the baseline in which the cells were completely separated was identified in order to calculate the difference ΔF (nN) to the maximum negative point of force.

Results showed that when cells were treated with ATPγS (100 μM) ($\mu = 1.6$nN ± 0.093, 95% CI [1.42, 1.786]), a 26.8% reduction in F_{max} occurred, in comparison to control ($\mu = 2.17$nN ± 0.077, 95% CI [2.023, 2.325]) (Figure 3, *A*, $P < 0.001$, 95% CI [0.287, 0.856]; Control: 27 cells, ATPγS: 19 cells, $n = 3$). This correlates to weakening of intercellular ligation forces as a consequence of diminished E-cadherin expression (Figure 2, *B*). To delineate a role for P2X7 in mediating these effects, cells were co-incubated with ATPγS +/– A438079 (50 μM). Mean value of F_{max} was increased to 2.45nN ± 0.085, 95% CI [2.284, 2.621] showing a restoration of cell–cell ligation forces when co-incubated with A438079 ($P < 0.001$, 95% CI [0.551, 1.148]; +A438079: 22 cells, $n = 3$). Box plots and histograms of the results are shown in Figure 3, *A* & *C* respectively.

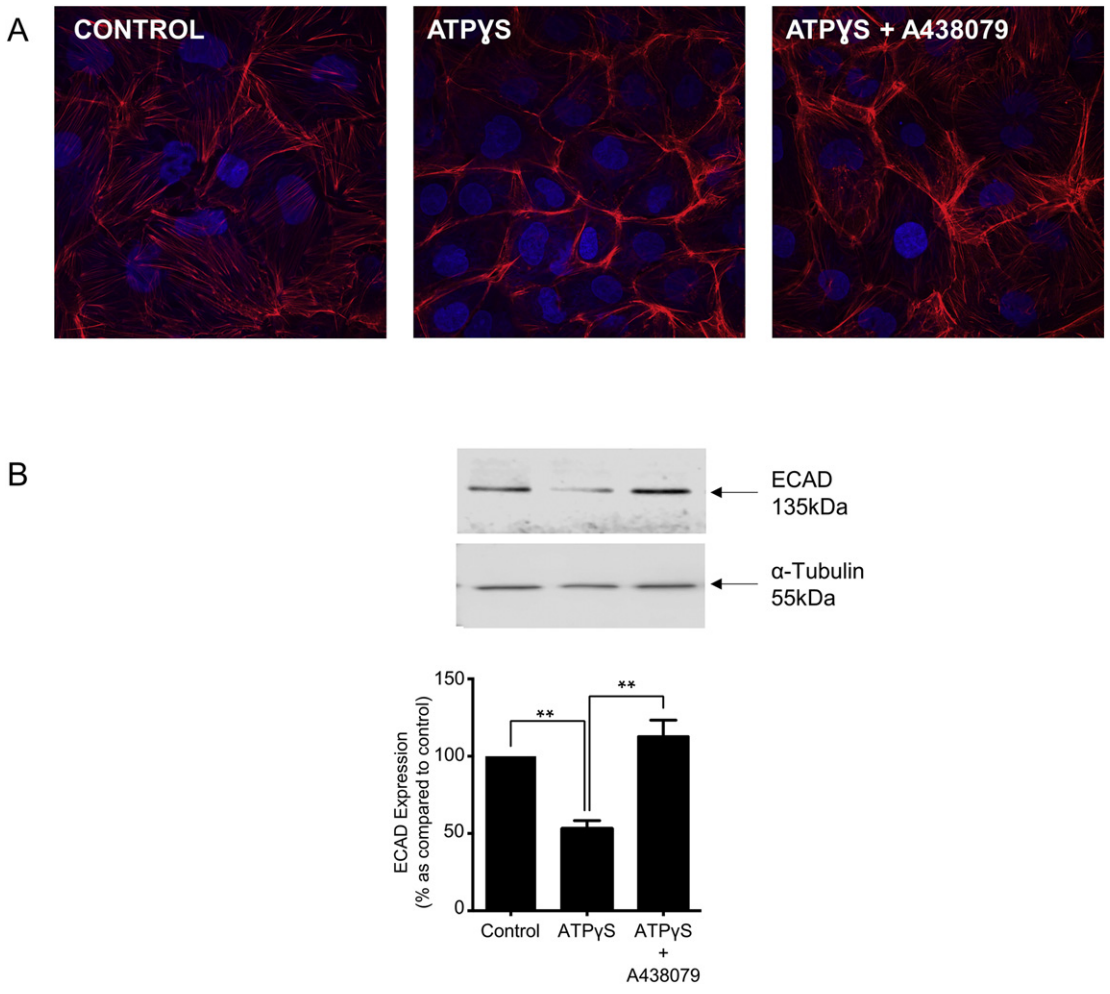

Figure 2. ATPγS down-regulates E-cadherin expression and induces cytoskeletal remodeling in proximal tubular epithelial cells. HK2 cells were cultured in 5 mM glucose for 48 h prior to an overnight serum-starvation, and subsequently incubated with ATPγS (100 μM) ± A438079 (50 μM) for 48 h. (**A**) Confocal microscopy of TRITC conjugated stained cells confirmed reorganization of the cytoskeleton in ATPγS treated cells, an effect negated when cells were co-incubated with P2X7 inhibitor A438079. (**B**) Western blot confirmed that incubation of HK2 cells with ATPγS (100 μM) ± A438079 (50 μM) for 48 h significantly decreased E-cadherin expression. Co-incubation with A438079 restored expression to control. Upper panel in **B** shows a representative blot for E-cadherin and α-tubulin as a loading control. Lower panel shows mean (± SEM) densitometry data, normalized against the non-stimulated low glucose control (100%), $n = 3$. Each lane in the representative blot corresponds to the associated bar in the graph.

ATPγS decreases tether rupture events (TREs) via activation of P2X7 receptors

Retraction *F-d* curves of soft cells have a unique pattern that resemble a step-like profile, corresponding to the unbinding of finite size adhesion clusters[20] that extend as displacement increases. In the early part of the separation process (10 μm) complex unbinding events occur ('*j*' events) that are preceded by a force ramp. As the pulling distance increases a plateau in the displacement indicates that membrane tethers extrude rupture of ligation clusters ('*t*' events). The number of tether rupture events (TREs) was detected by identifying sharp steps of force that correspond to cluster ruptures.[31] The retraction *F-d* curve of Figure 4, *B* illustrates the number of TREs as detected by the step fitting function. During the continuous pulling speed only upwards events are anticipated, hence only positive steps were detected to avoid drifts of the cantilevers.

Analysis of retraction *F-d* curves showed that ATPγS (100 μM) treated cells ($\mu = 44.69 \pm 2.4$, 95% CI [39.989, 49.382]), exhibit a 22.3% reduction in the number of TRES compared to control ($\mu = 57.49 \pm 2.0$, 95% CI [53.508, 61.478]), (Figure 4, *A*, $P < 0.001$, 95% CI [5.432, 20.184]; Control: 25 cells, ATPγS: 18 cells, $n = 3$). Coincubation with ATPγS ± A438079 ($\mu = 68.75 \pm 2.2$, 95% CI [64.436, 73.064]) restored the number of the rupture events, increasing TREs by 53.84% as compared to ATPγS alone ($P < 0.001$, 95% CI [16.428, 31.702]; +A438079: 22 cells, $n = 3$). These data are in agreement with F_{max} and E-cadherin expression results. Box plots and histograms of the results are shown in Figure 4, *A & C* respectively.

ATPγS decreases the work of adhesion (Wd) via activation of P2X7 receptors

The total energy consumed during the pulling process prior to complete separation (defined as the baseline above), was calculated by the integration of the retraction *F-d* curve and is referred as the work of adhesion W_d. Since the pulling force is

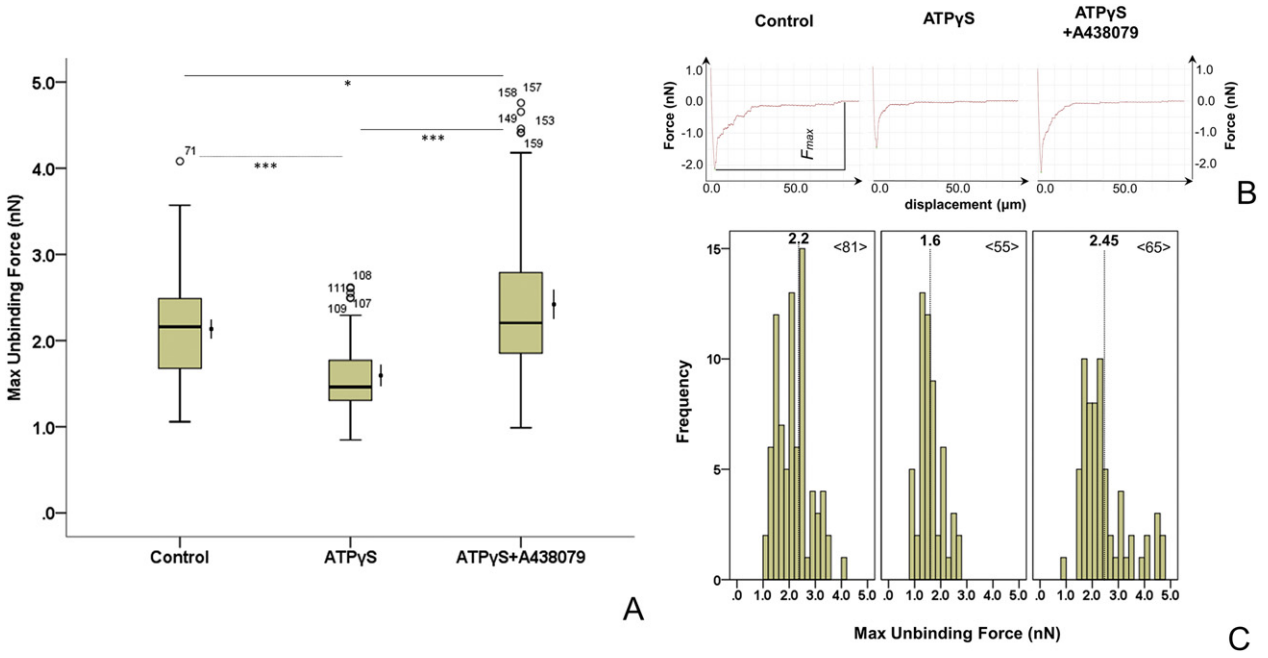

Figure 3. (**A**) The maximum unbinding force F_{max} of HK2 cells treated with ATPγS (100 μM) ± A438079 (50 μM) for 48 h is shown. The values inside the box represent the first (lower value) and third quartile, the line within the box represents the median, the bars show the minimum and maximum observations and the (o) indicates the outliers. The line outside of the box shows the mean and the 95% confidence interval range. (**B**) Indicative retraction curves from each treatment. F_{max} is the maximum negative point and is calculated by subtraction from the baseline. (**C**) Histograms of F_{max} showing the frequency distribution of the retraction data from each treatment. The number of analyzed F-*d* curves is given in the histograms, <F-*d*>. The dotted line represents the mean value.

integrated over the separated distance (gray area in Figure 5, *B*), W_d is driven by molecular changes in E-cadherin ligation and F-actin cytoskeleton.

Results showed that ATPγS (100 μM) treated cells (μ = 13.32fJ ± 1.13, 95% CI [10.702, 15.93]) exhibited a 39.04% reduction in W_d compared to control (μ = 21.85fJ ± 1.1, 95% CI [19.677, 24.013]), (Figure 5, *A*, $P < 0.001$, 95% CI [4.462, 12.596]; Control: 27 cells, ATPγS: 19 cells, $n = 3$), an effect negated when co-incubated with the P2X7 antagonist (μ = 23.73fJ ± 1.22, 95% CI [21.323, 26.133]). Coincubation with ATPγS ± A438079 (μ = 23.73 ± 1.219, 95% CI [21.323, 26.133]) restored the work of adhesion as compared to ATPγS alone ($P < 0.001$, 95% CI [6.158, 14.665]; +A438079: 22 cells, $n = 3$). No statistical significance between control and + A438079 was found. Box plots and histograms of the results are shown in Figure 5, *A* & *C* respectively.

Discussion

Hemichannel-mediated release of ATP into the intercellular space around tubular epithelial cells of the diabetic kidney has been linked to disease progression.[8] Understanding the effects of ATP in exacerbating the loss of cell–cell adhesion is fundamental to advancing therapeutic strategies that may help alleviate the effects of this debilitating complication. Nanoscale force-displacement measurements provide a multi-variable signature of the cell–cell separation process that captures the complexity of the adherens junction and its integrated response to purinergic receptor activation. We have used SCFS to investigate the effects of ATPγS on cell–cell adhesion in renal proximal tubule (HK2) epithelial cells. The HK2 cell line maintains functional characteristics of human proximal tubular epithelium and has been previously used to characterize alterations in E-cadherin mediated cell–cell adhesion.[3,6] The organization of surface ligation bindings into finite sized clusters is evidenced by the step-like pattern of the retraction curve. After initial cell–cell contact, a variety of processes, such as junction formation and intercellular signaling are initiated.[16] The initial recognition event involves the formation of *trans*-dimers between cadherin monomers located on the interface of junctional contact followed by the clustering of cadherin into larger structures to form adhesion.[33,34] The organization of E-cadherin in to clusters depends on links with cytoskeleton.[19,34] SCFS has the advantage of functional characterization of adhesion at the cellular level by examining E-cadherin ligation at the EC domain in correlation with the machinery that regulates its function.[35] Adhesion parameters derived from separation experiments showed a variable response to integrated changes of the AJ-CSK architecture. As evidenced by changes in F_{max} and TREs, the AJ-CSK complex regulates cell adhesion by physico-chemical modulation of the number of competent ligations and associated clustering organization. Changes in mechanical properties of cells, due to cytoskeletal re-organization, affect their separation response by modulating deformation as shown by changes in W_d. Previous data suggest that single cell mechanics strongly correlate with changes in the adhesion energy rather than binding forces at the whole cell level.[6]

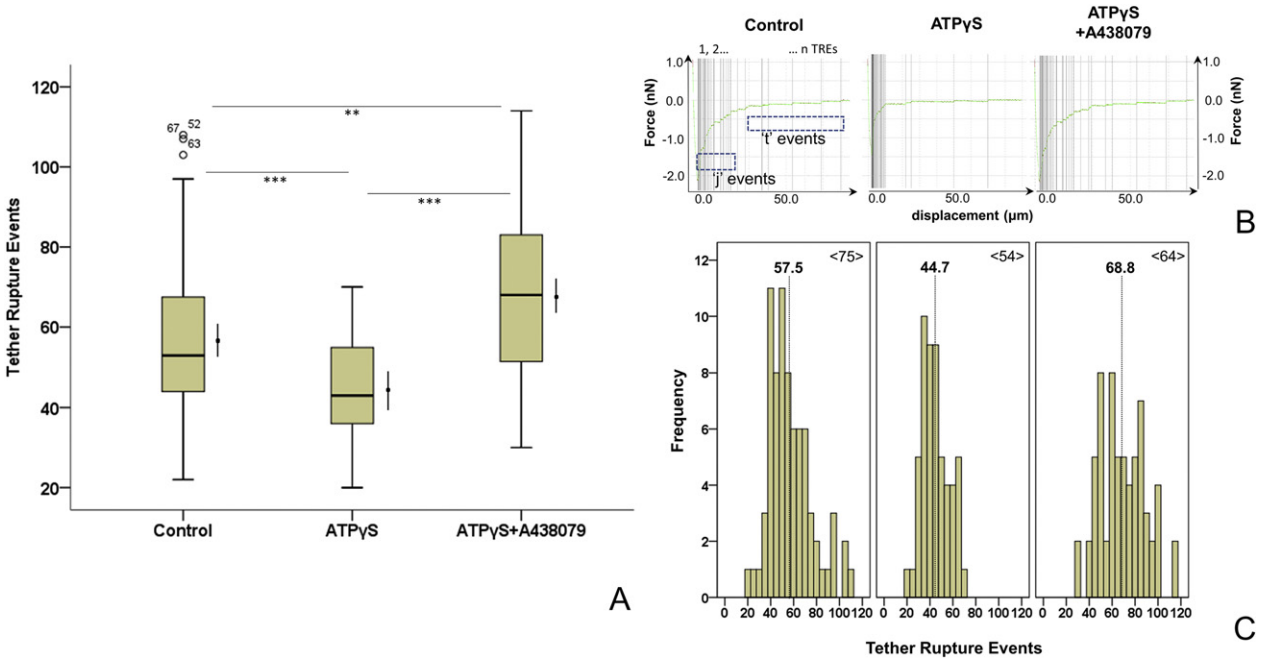

Figure 4. (**A**) The number of tether rupture events (TREs) of HK2 cells treated with ATPγS (100 μM) ± A438079 (50 μM) for 48 h is shown. A step fitting algorithm was fitted to the point right of the minimum value (F_{max} point). The line outside of the box shows the mean and the 95% confidence interval range. (**B**) Indicative retraction curves from each treatment. Total number of TREs over the distance of separation is shown. (**C**) Histograms of TREs showing the frequency distribution of the retraction data from each treatment. The number of analyzed F-*d* curves is given in the histograms, <F-*d*>. The dotted line represents the mean value.

The concentration of ATP in the cytoplasm of cells is high (1-10 mM), while levels in the extracellular space are extremely low, ranging between 1 and 10 nM.[36] In diabetic nephropathy, glucose-evoked TGFβ1 increases hemichannel-mediated ATP release.[8] Designed to maintain cellular communication following a loss in gap junction intercellular communication in disease, the local rise in ATP activates P2X7 receptors to exacerbate renal injury.[13,37] In the current study, we present novel evidence that treatment of HK2 cells with ATPγS dramatically reduces all adhesion parameters measured. The maximum unbinding force is the force required to break ligation between E-cadherin clusters on coupled cells. Reduction of F_{max} clearly suggests that the number of cadherin dimers was reduced after P2X7 activation in agreement with whole cell expression of E-cadherin. In addition, ATPγS reduced the number of tether rupture events, suggesting that the number of competent binding molecules available to form clusters was reduced and the organizational function of ligation was compromised, a finding in agreement with reduced unbinding forces, E-cadherin expression and cytoskeletal re-organization. Mean values showed a negative percentage change of 26.8% and 22.6% for F_{max} and TREs respectively. Reduced rupturing between cadherin clusters demonstrates the inability of ATPγS-treated cells to organize binding molecules into clusters to ensure appropriate ligation. Evidence in the literature suggests that this loss of this function is associated with cytoskeletal re-organization.[18,20,32,33] The work of detachment (W_d) was reduced dramatically (39%) after ATPγS treatment. Considering that actin polymerization mostly affects W_d during separation due to mechanics,[6,38] the considerable loss in work of detachment in comparison to unbinding force (39% vs 27%) can be explained by changes in the cytoskeleton after treatment rather than any effects on the extracellular interface associated with ligation. Therefore, apart from its role to reinforce ligation clustering, re-arrangement of the cytoskeleton into peripheral stress fibers biophysically affected the work of detachment. This is clearly shown in *F-d* curves, where W_d is a function of maximum unbinding forces and the last unbinding event, which is a measure of distance. As a result, the underlying molecular machinery associated with the determination of cell deformation during separation, involved changes in both surface avidity and actin cytoskeleton, with the latter dominating the process as shown by SCFS.

Cytoskeletal reorganization following ATPγS treatment affected biophysically the work of detachment and molecularly the organization of ligation clustering. Inhibition of P2X7 restored cell–cell adhesion. Force-displacement (*F-d*) retraction curves suggest that membrane molecular binding and architecture of the AJ-CSK complex were re-established; F_{max} and TREs were significantly increased (53%) in agreement with an increase in whole cell expression, suggesting that the number of competent adhesion ligations and clustering organization was restored, in correlation with a markedly increase in W_d (78%) after P2X7 inhibition. Biophysically, restoration of the deformation ability of cells after cytoskeletal polymerization explains the increase in W_d. Determining strength of adhesion in disease

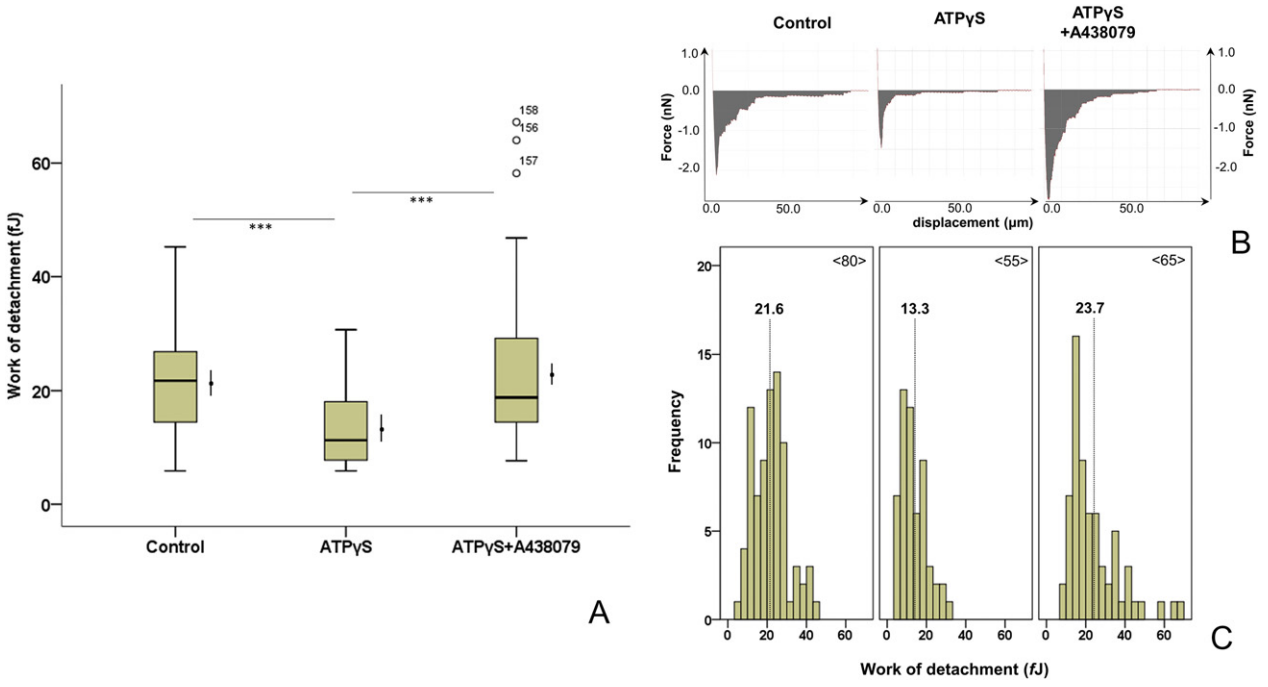

Figure 5. (**A**) The work of complete detachment W_d of HK2 cells treated with ATPγS (100 μM) ± A438079 (50 μM) for 48 h is shown. The values inside the box represent the first (lower value) and third quartile, the line within the box represents the median, the bars show the minimum and maximum observations and the (o) indicates the outliers. The line outside of the box shows the mean and the 95% confidence interval range. (**B**) Indicative retraction curves from each treatment. W_d is a function of the pulling force integrated over the separated distance. (**C**) Histograms of W_d showing the frequency distribution of the retraction data from each treatment. The number of analyzed F-*d* curves is given in the histograms, <F-*d*>. The dotted line represents the mean value.

is challenging due to the underlying molecular assembly that regulates AJ formation. Force-displacement measurements during cell–cell separation can provide valuable information about the response to ligands and their antagonists. Nanoscale SCFS retraction curves capture the molecular activity underlying ATP evoked changes in cell adhesion, loss of which appears to be mediated by downstream P2X7 receptor activation and supports a role for P2X7 as a potential therapeutic target in managing progression of diabetic nephropathy.

References

1. Methven S, Steenkamp R, Fraser S. UK renal registry 19th annual report: chapter 5 survival and causes of death in UK adult patients on renal replacement therapy in 2015: national and centre-specific analyses. *Nephron* 2017;**137**:117-50.
2. Zeisberg M, Neilson EG. Mechanisms of tubulointerstitial fibrosis. *J Am Soc Nephrol* 2010;**21**:1819-34.
3. Hills CE, Siamantouras E, Smith SW, Cockwell P, Liu KK, Squires PE. TGFβ modulates cell-to-cell communication in early epithelial-to-mesenchymal transition. *Diabetologia* 2012;**55**:812-24.
4. Hills CE, Squires PE. TGF-β1-induced epithelial-to-mesenchymal transition and therapeutic intervention in diabetic nephropathy. *Am J Nephrol* 2010;**31**:68-74.
5. Hills CE, Squires PE. The role of TGF-β and epithelial-to mesenchymal transition in diabetic nephropathy. *Cytokine Growth Factor Rev* 2011;**22**:131-9.
6. Siamantouras E, Hills CE, Squires PE, Liu K-K. Quantifying cellular mechanics and adhesion in renal tubular injury using single cell force spectroscopy. *Nanomedicine* 2016;**12**:1013-21.
7. Hills CE, Price GW, Squires PE. Mind the gap: connexins and cell-cell communication in the diabetic kidney. *Diabetologia* 2015;**58**:233-41.
8. Hills CE, Price GW, Wall MJ, Kaufmann TJ, Tang SC, Yiu WH, et al. Transforming growth factor beta 1 drives a switch in connexin mediated cell-to-cell communication in tubular cells of the diabetic kidney. *Cell Physiol Biochem* 2018;**45**:2369-88.
9. Geraghty NJ, Watson D, Sluyter R. Long-term treatment with the P2X7 receptor antagonist brilliant blue G reduces liver inflammation in a humanized mouse model of graft-versus-host disease. *Cell Immunol* 2019;**336**:12-9.
10. Thawkar BS, Kaur G. Inhibitors of NF-κB and P2X7/NLRP3/Caspase 1 pathway in microglia: novel therapeutic opportunities in neuroinflammation induced early stage Alzheimer's disease. *J Neuroimmunol* 2019;**326**:62-74.
11. Tung HC, Lee FY, Wang SS, Tsai MH, Lee JY. Huo TI, et al. The beneficial effects of P2X 7 antagonism in rats with bile duct ligation-induced cirrhosis. *PloS ONE* 2015;**1**e0124654.
12. Wang C, Hou XX, Rui HL, Li LJ, Zhao J, Yang M, et al. Artificially cultivated Ophiocordyceps sinensis alleviates diabetic nephropathy and its podocyte injury via inhibiting P2X7 expression and NLRP3 inflammasome activation. *J Diabetes Res* 2018;**11**1390418.
13. Menzies RI, Booth JWR, Mullins JJ, Bailey MA, Tam FWK, Norman JT, et al. Hyperglycemia-induced renal P2X7 receptor activation enhances diabetes-related injury. *EBioMedicine* 2017;**19**:73-83.
14. Kreft E, Kowalski R, Jankowski M, Szczepańska-Konkel M. Renal vasculature reactivity to agonist of P2X7 receptor is increased in streptozotocin-induced diabetes. *Pharmacol Rep* 2016;**68**:71-4.
15. Menzies RI, Tam FW, Unwin RJ, Bailey MA. Purinergic signaling in kidney disease. *Kidney Int* 2017;**91**:315-23.
16. Bajpai S, Correia J, Feng Y, Figueiredo J, Sun SX, Longmore GD, et al. (2008) alpha-Catenin mediates initial E-cadherin-dependent cell-cell

recognition and subsequent bond strengthening. *Proc Natl Acad Sci U.S. A* 2008;**105**:18331–36.
17. Meng W, Takeichi M. Adherens junction: molecular architecture and regulation. *Cold Spring Harb Perspect Biol* 2009;**1**(6):a002899.
18. Chen CS, Hong S, Indra I, Sergeeva AP, Troyanovsky RB, Shapiro L, et al. A-catenin-mediated cadherin clustering couples cadherin and actin dynamics. *J Cell Biol* 2015;**210**:647-61.
19. Hong S, Troyanovsky RB, Troyanovsky SM. Binding to F-actin guides cadherin clustering assembly, stability and movement. *J Cell Biol* 2013;**201**:131-43.
20. Wu Y, Kanchanawong P, Zaidel-Bar R. Actin-delimited adhesion-independent clustering of E-cadherin forms the nanoscale building blocks of adherens junctions. *Dev Cell* 2015;**32**:139-54.
21. Maitre JL, Heisenberg CP. Three functions of cadherins in cell adhesion. *Curr Biol Rev* 2013;**23**:R626-33.
22. Hills CE, Jin T, Siamantouras E, Liu K-K, Jefferson KP, Squires PE, et al. a loss of cell-to-cell adhesion in proximal tubule-derived cells: modulation of the adherens junction complex by ketamine. *PLoS ONE* 2013;**8**(8)e71819.
23. Andolfi L, Bourkoula E, Migliorini E, Palma A, Pucer A, Skrap M, et al. Investigation of adhesion and mechanical properties of human glioma cells by single cell force spectroscopy an atomic force microscopy. *PLoS ONE* 2014;**9**(11)e112582.
24. Omidvar R, Tafazzoli-shadpour M, Shokrgozar MA, Rostami M. Atomic force microscope-based single cell force spectroscopy of breast cancer lines: an approach for evaluating cellular invasion. *J Biomech* 2014;**47**:3373-9.
25. Harris TJ, Tepass U. Adherens junctions: from molecules to morphogenesis. *Nat Rev Mol Cell Biol* 2010;**11**:502-14.
26. Benoit M, Gabriel D, Gerisch G, Gaub HE. Discrete interactions in cell adhesion measured by single-molecule force spectroscopy. *Nat Cell Biol* 2000;**2**:313-7.
27. Friedrichs J, Legate KR, Schubert R, Bharadwaj M, Werner C, Muller DJ, et al. A practical guide to quantify cell adhesion using single-cell force spectroscopy. *Methods* 2013;**60**:169-78.
28. Kashef J, Franz CM. Quantitative methods for analysing cell-cell adhesion in development. *Dev Biology* 2015;**401**:165-74.
29. Hutter JL, Bechhoefer J. Calibration of atomic-force microscope tips. *Rev Sci Instrum* 1993;**64**(7):1868-73.
30. Butt HJ, Jaschke M. Calculation of thermal noise in atomic force microscopy. *Nanotechnology* 1995;**6**(1):1-7.
31. Kerssemakers JWJ, Munteanu EL, Laan L, Noetzel TL, Janson ME, Dogterom M. Assembly dynamics of microtubules at molecular resolution. *Nature* 2006;**442**:709-12.
32. Zhang Y, Sivasankar S, Nelson WJ, Chu S. Resolving cadherin interactions and binding cooperativity at the single-mole level. *Proc Natl Acad Sci U S A* 2009;**106**:109-14.
33. Pontani LL, Jorjadze I, Brujic J. Cis and trans cooperativity of E-cadherin mediates adhesion in biomimetic lipid droplets. *Biophys J* 2016;**110**:391-9.
34. Baum B, Georgiou M. Dynamics of adherens junctions in epithelial establishment. *maintenance and remodelling J Cell Biol* 2011;**192**:907-17.
35. Friedrichs J, Helenius J, Muller DJ. Quantifying cellular adhesion to extracellular matrix components by single-cell force spectroscopy. *Nat Protocols* 2010;**5**:1353-61.
36. Vitiello L, Gorini S, Rosano G, la Sala A. Immunoregulation through extracellular nucleotides. *Blood* 2012;**120**:511-8.
37. Rabadi M, Kim M, Li H, Han SJ, Choi Y, D'Agati V, et al. ATP induces PAD4 in renal proximal tubule cells via P2X7 receptor activation to exacerbate ischemic AKI. *Am J Physiol Renal Physiol* 2018;**314**: F293-305.
38. Siamantouras E, Hills CE, Younis MGY, Squires PE, Liu K-K. Quantitative investigation of calcimimetic R568 on beta cell adhesion and mechanics using AFM single-cell force spectroscopy. *FEBS Lett* 2014;**588**:1178-83.